Acta Cryst. (1982). B38, 2312–2315

Structure of the Tri-*o*-thymotide–Ethyl Methyl Sulfoxide (2:1) Clathrate.* Crystallographic Estimation of the Enantioselectivity

BY J. ALLEMAND AND R. GERDIL†

Département de Chimie Organique et Laboratoire de Radiocristallographie, Université de Genève, 30 quai Ernest Ansermet, 1211 Genève, Switzerland

(*Received* 9 *December* 1981; *accepted* 29 *March* 1982)

Abstract. $C_{33}H_{36}O_6.\frac{1}{2}C_3H_8OS$, trigonal, $P3_121$, a = 13·538 (3), c = 30·598 (16) Å, Z = 6, D_m = 1·177, D_x = 1·179 Mg m^{-3}, μ = 0·1154 mm^{-1}. Data were collected at room temperature. Final R = 0·049 for 935 observed reflections. The present structure analysis is mainly concerned with the determination, by crystallographic means only, of the enantiomeric ratio of the caged ethyl methyl sulfoxide (EMSO) molecules in a single crystal of the tri-*o*-thymotide (TOT) clathrate.

Introduction. The present X-ray investigation is part of a more general stereochemical study of the enantioselective inclusion properties exhibited by TOT clathrates towards certain chiral guest molecules (Gerdil & Allemand, 1980; Gerdil, Allemand & Bernardinelli, 1981).

Single crystals of the clathrate were grown from pure racemic material by slow cooling. Two types of habits, both having the same cell dimensions, were isolated: hexagonal {110}/{001} prisms, and trigonal prisms displaying the symmetry of the enantiomorphous class 32. A crystal 0·35 × 0·35 × 0·34 mm was selected from those of the symmetry class 32 and used for all the measurements. Lattice parameters and diffracted intensities were obtained with a four-circle Philips PW1100 diffractometer (graphite monochromator, Mo $K\alpha$ radiation, ω–2θ scan). 1975 non-unique reflections were scanned in the range $3° < \theta < 16°$. After averaging pairs of equivalent reflections 935 unique structure amplitudes for space group $P3_121$ had $|F_o| > 2\sigma(F_o)$ and were used in the structure analysis. The cage-type clathrates are isomorphous, therefore the host structure was refined starting from the coordinates of the non-H atoms of the TOT–2-bromobutane clathrate (Allemand & Gerdil, 1982). The (*M*) configuration was arbitrarily assigned to the TOT molecule. A ΔF synthesis disclosed the (*R*) configuration of EMSO in its twofold positional disorder in accordance with the imposed local symmetry of the cage. The two equivalent S atoms are separated by 1·58 Å, whereas the O atoms lie near the symmetry axis, at a short distance (0·33 Å) from each other (see Fig. 4). No peak of significant intensity revealed the location of the disordered methylene groups. In order to make up for the lack of a reasonable structure for the guest molecule the relevant internal molecular parameters were taken from the geometry of *meso*-1,2-bis-(methylsulfinyl)ethane (Svinning, Mo & Bruun, 1976). The resulting conformation (Fig. 1*b*; Table 2) was included as a *rigid component* in the X-ray structure model. An overall isotropic temperature factor was assigned to the guest in the subsequent refinements. A ΔF synthesis revealed the position of most of the H atoms of TOT. The optimized orientation of the alkyl substituents was determined in a similar manner to the structure analysis of TOT–2-bromobutane (Allemand & Gerdil, 1982). The structure model (*M*)-TOT–(*R*)-EMSO (2:1) was refined anisotropically (isotropically for the H atoms and the rigid guest component) by least-squares analysis to an R value of 0·054. A unit weight was assigned to each of the 1006 included reflections with the conditions $|F_o| > 2\sigma(F_o)$; and when $|F_o| \leq 2\sigma(F_o)$ only if $|F_c| > |F_o|$. A similar refinement, to a convergence limit of R = 0·17, was simultaneously carried out for a second structure model consisting of the host molecule only. Difference syntheses were calculated on the basis of both preceding models but, in the former case, with F_c from which the contribution of EMSO had been omitted. Sections through the difference electron-density distribution around the disordered S atoms are shown in Fig. 2. Apart from inherent differences due to the scale factors the deformations of the electron-density distribution are very much alike in both maps, thus demonstrating that no bias is introduced by the inclusion of the guest in the model prior to refinement. It was important to assess this point before attempting to interpret the changes engendered in the residual electron-density maps (see below) by varying the (*R*) to (*S*) enantiomeric ratio in the F_c model.

* *o*-Thymotic acid is 2-hydroxy-3-isopropyl-6-methylbenzoic acid.

† To whom correspondence should be addressed.

0567-7408/82/082312-04$01.00

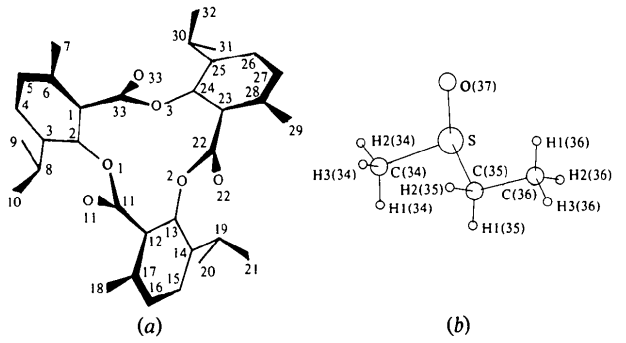

(*a*) (*b*)

Fig. 1. The atom-numbering system: (*a*) idealized (*M*) configuration of (−)-tri-*o*-thymotide; (*b*) model for (*R*)(−)-ethyl methyl sulfoxide used as a rigid conformer in the refinements.

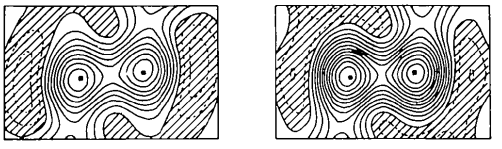

(*a*) (*b*)

Fig. 2. Sections through three-dimensional ΔF syntheses in the plane containing the axially disordered S atoms (■) of (*R*)-ethyl methyl sulfoxide. Contours at intervals of 1 e Å^{-3}; negative contours dashed. (*a*) Calculated on the basis of the refined model (*M*)-TOT–(*R*)-EMSO (2:1) with F_c from which the contribution of the guest had been omitted; (*b*) F_c calculated from the host structure refined to convergence limit without inclusion of the guest.

Estimation of the (R) to (S) enantiomeric ratio of EMSO. Since a cage can accommodate at most one guest molecule, the 'stoichiometry' of the cage-type TOT complexes is formally characterized by the ratio of the number ($Z = 6$) of TOT molecules to the number ($Z' = 3$) of accessible cages in the unit cell. This ratio is independent of the actual occupancy factor of the guest and serves well to characterize the cage clathrates of TOT. The occurrence of non-stoichiometric host:guest ratios in several TOT clathrates was pointed out by Powell (1964). Indeed vacant cavities were detected by various methods in most of the clathrates that we have investigated so far. Accurate values for the guest occupancy factor are not readily obtained and are, in addition, subject to variations depending on the conditions of growth of the crystal. An *average* population parameter of 0·96, determined by NMR analysis, was taken as representative for the crystal used in the present study.

Difference syntheses were further used to detect the presence of the (*S*) enantiomer by taking advantage of the higher scattering power of the S atom. The F_c values were calculated on the basis of the following structure model: (*M*)-TOT–(*R*)-EMSO/(*S*)-EMSO ($2{:}x_R{:}x_S$), where the adjustable population parameters x_R and x_S are subject to the restriction $x_R + x_S \leq 1$. The molecular components of the F_c model were

Table 1. *Atomic coordinates and isotropic temperature factors* ($\times 10^3$) *of TOT*

U_{eq} (Å^2) $= \frac{1}{3} \sum_i \sum_j U_{ij} a_i^* a_j^* (\mathbf{a}_i . \mathbf{a}_j)$.

	x	y	z	U_{eq}
O(1)	0·9756 (6)	0·3297 (7)	0·3915 (4)	48 (5)
O(2)	0·8756 (6)	0·4668 (5)	0·4043 (2)	51 (4)
O(3)	0·8148 (5)	0·3371 (5)	0·3278 (2)	49 (4)
O(11)	0·8802 (8)	0·2038 (9)	0·4450 (3)	91 (6)
O(22)	0·7107 (6)	0·3669 (7)	0·4406 (2)	89 (5)
O(33)	0·6821 (7)	0·1632 (7)	0·3513 (3)	117 (6)
C(1)	0·869 (1)	0·197 (1)	0·3336 (6)	46 (8)
C(2)	0·965 (2)	0·244 (1)	0·3616 (4)	45 (9)
C(3)	1·052 (1)	0·220 (1)	0·3574 (5)	60 (10)
C(4)	1·044 (1)	0·147 (1)	0·3230 (6)	65 (9)
C(5)	0·948 (2)	0·100 (1)	0·2956 (5)	71 (9)
C(6)	0·861 (1)	0·123 (1)	0·3007 (5)	50 (9)
C(7)	0·759 (1)	0·068 (1)	0·2723 (4)	73 (8)
C(8)	1·153 (1)	0·267 (1)	0·3891 (4)	70 (8)
C(9)	1·263 (1)	0·320 (1)	0·3626 (4)	90 (8)
C(10)	1·140 (1)	0·176 (1)	0·4208 (4)	91 (9)
C(11)	0·933 (1)	0·301 (1)	0·4326 (5)	60 (10)
C(12)	0·9653 (9)	0·406 (1)	0·4587 (3)	43 (7)
C(13)	0·9382 (9)	0·487 (1)	0·4431 (4)	45 (7)
C(14)	0·9778 (9)	0·592 (1)	0·4648 (3)	51 (7)
C(15)	1·0440 (9)	0·609 (1)	0·5026 (4)	58 (7)
C(16)	1·069 (1)	0·530 (1)	0·5170 (3)	63 (8)
C(17)	1·030 (1)	0·426 (1)	0·4964 (3)	56 (8)
C(18)	1·062 (1)	0·342 (1)	0·5128 (4)	85 (8)
C(19)	0·950 (1)	0·678 (1)	0·4477 (4)	72 (8)
C(20)	1·057 (2)	0·788 (1)	0·4355 (5)	150 (10)
C(21)	0·881 (1)	0·706 (1)	0·4791 (4)	130 (10)
C(22)	0·7592 (9)	0·4089 (9)	0·4073 (4)	57 (7)
C(23)	0·708 (1)	0·411 (1)	0·3653 (5)	47 (8)
C(24)	0·731 (1)	0·372 (1)	0·3274 (7)	49 (7)
C(25)	0·685 (1)	0·373 (1)	0·2871 (6)	50 (8)
C(26)	0·609 (1)	0·410 (1)	0·2857 (4)	61 (8)
C(27)	0·581 (1)	0·451 (1)	0·3234 (7)	68 (8)
C(28)	0·630 (1)	0·452 (1)	0·3640 (5)	55 (8)
C(29)	0·603 (1)	0·500 (1)	0·4033 (4)	95 (9)
C(30)	0·714 (1)	0·330 (1)	0·2451 (5)	74 (9)
C(31)	0·775 (1)	0·428 (1)	0·2124 (4)	91 (9)
C(32)	0·604 (1)	0·233 (1)	0·2250 (4)	102 (9)
C(33)	0·7788 (9)	0·2300 (9)	0·3394 (3)	60 (7)

Table 2. *Atomic coordinates of the rigid models for (R)- and (S)-ethyl methyl sulfoxide*

(*R*) model: population parameter 0·44. The mean e.s.d.'s are: for x and y 2×10^{-3}, for z 8×10^{-4}.

(*S*) model: population parameter 0·04. The mean e.s.d.'s are: for x and y 8×10^{-3}, for z 3×10^{-3}.

The overall isotropic temperature factor is 0·144 (1) Å^2.

		x	y	z
S	*R*	0·2964	−0·0036	0·3075
C(34)	*R*	0·2697	−0·1466	0·3034
C(35)	*R*	0·4062	0·0443	0·3486
C(36)	*R*	0·4409	0·1651	0·3620
O(37)	*R*	0·1943	−0·0099	0·3295
S	*S*	0·2736	−0·0918	0·3443
C(34)	*S*	0·4263	0·1219	0·3716
C(35)	*S*	0·3961	0·0448	0·3320
C(36)	*S*	0·2564	−0·1525	0·2910
O(37)	*S*	0·1760	−0·0707	0·3511

positioned as follows: the coordinates (as well as the thermal parameters) of the TOT and (*R*)-EMSO molecules were those resulting from the final refinement ($R = 0.054$) of the starting model (*M*)-TOT–(*R*)-EMSO (2:1). The orientation of the (*S*) enantiomer was calculated by the use of the *PCK*-6 program (Williams, 1972). Representative difference density maps are reported in Fig. 3. Following the inclusion of the (*R*) enantiomer only (Fig. 3*a*), distinct peaks appear at the calculated locations of the S atom of the missing (*S*) enantiomer. In addition, negative troughs near the S-atom positions of the (*R*) enantiomer indicate that too much electron density is provided by the S atom of the F_c model. A substantial decrease of the enantiomeric excess (e.e.) to 72% inverts the preceding situation (Fig. 3*c*), thus fixing a lower limit for the contribution of the (*R*) enantiomer. Stepwise complementary adjustments of the population parameters led to the values 0·88 and 0·08 for x_R and x_S respectively. In the corresponding difference map (e.e. 83%; Fig. 3*b*) the electron density is evenly distributed between the two non-equivalent S-atom positions, with peak heights of 2·1 and 1·7 e Å^{-3} for the (*R*) and (*S*) enantiomer respectively. Refinement of the latter model with a common isotropic thermal parameter for both enantiomeric rigid bodies decreased

Table 3. *Bond distances* (Å) *and angles* (°) *in TOT and EMSO*

O(1)–C(2)	1·421 (19)	C(13)–C(14)	1·409 (19)
O(1)–C(11)	1·355 (19)	C(14)–C(15)	1·409 (16)
O(2)–C(13)	1·406 (14)	C(14)–C(19)	1·497 (23)
O(2)–C(22)	1·367 (12)	C(15)–C(16)	1·356 (25)
O(3)–C(24)	1·434 (18)	C(16)–C(17)	1·381 (22)
O(3)–C(33)	1·326 (13)	C(17)–C(18)	1·489 (25)
O(11)–C(11)	1·203 (19)	C(19)–C(20)	1·522 (18)
O(22)–C(22)	1·192 (13)	C(19)–C(21)	1·506 (25)
O(33)–C(33)	1·217 (12)	C(22)–C(23)	1·471 (21)
C(1)–C(2)	1·412 (24)	C(23)–C(24)	1·376 (26)
C(1)–C(6)	1·388 (24)	C(23)–C(28)	1·404 (25)
C(1)–C(33)	1·512 (26)	C(24)–C(25)	1·378 (27)
C(2)–C(3)	1·387 (31)	C(25)–C(26)	1·366 (26)
C(3)–C(4)	1·407 (26)	C(25)–C(30)	1·535 (24)
C(3)–C(8)	1·532 (21)	C(26)–C(27)	1·408 (25)
C(4)–C(5)	1·399 (25)	C(27)–C(28)	1·407 (25)
C(5)–C(6)	1·370 (32)	C(28)–C(29)	1·499 (22)
C(6)–C(7)	1·479 (20)	C(30)–C(31)	1·531 (18)
C(8)–C(9)	1·518 (19)	C(30)–C(32)	1·533 (17)
C(8)–C(10)	1·511 (22)	S–C(34)	1·787*
C(11)–C(12)	1·490 (23)	S–C(35)	1·802*
C(12)–C(13)	1·400 (24)	S–O(37)	1·501*
C(12)–C(17)	1·394 (15)	C(35)–C(36)	1·515*
C(2)–O(1)–C(11)	120·5 (11)	C(12)–C(17)–C(16)	117·4 (16)
C(13)–O(2)–C(22)	117·6 (8)	C(12)–C(17)–C(18)	121·6 (13)
C(24)–O(3)–C(33)	116·5 (8)	C(16)–C(17)–C(18)	120·9 (11)
C(2)–C(1)–C(6)	119·1 (19)	C(14)–C(19)–C(20)	111·1 (14)
C(2)–C(1)–C(33)	119·5 (16)	C(14)–C(19)–C(21)	113·7 (11)
C(6)–C(1)–C(33)	121·4 (14)	C(20)–C(19)–C(21)	108·3 (13)
O(1)–C(2)–C(1)	117·2 (19)	O(2)–C(22)–O(22)	122·3 (11)
O(1)–C(2)–C(3)	120·0 (13)	O(2)–C(22)–C(23)	110·5 (9)
C(1)–C(2)–C(3)	122·4 (15)	O(22)–C(22)–C(23)	127·2 (10)
C(2)–C(3)–C(4)	117·2 (14)	O(22)–C(23)–C(24)	121·8 (15)
C(2)–C(3)–C(8)	122·2 (15)	C(22)–C(23)–C(28)	119·2 (14)
C(4)–C(3)–C(8)	120·6 (18)	C(24)–C(23)–C(28)	119·0 (15)
C(3)–C(4)–C(5)	120·1 (19)	O(3)–C(24)–C(23)	119·3 (16)
C(4)–C(5)–C(6)	122·0 (15)	O(3)–C(24)–C(25)	116·1 (16)
C(1)–C(6)–C(5)	119·1 (14)	C(23)–C(24)–C(25)	124·3 (15)
C(1)–C(6)–C(7)	120·3 (17)	C(24)–C(25)–C(26)	117·1 (15)
C(5)–C(6)–C(7)	120·6 (14)	C(24)–C(25)–C(30)	123·5 (15)
C(3)–C(8)–C(9)	108·7 (11)	C(26)–C(25)–C(30)	119·4 (15)
C(3)–C(8)–C(10)	110·2 (10)	C(25)–C(26)–C(27)	121·3 (15)
C(9)–C(8)–C(10)	114·7 (15)	C(26)–C(27)–C(28)	120·6 (16)
O(1)–C(11)–O(11)	122·9 (15)	C(23)–C(28)–C(27)	117·7 (15)
O(1)–C(11)–C(12)	110·2 (12)	C(23)–C(28)–C(29)	122·6 (14)
O(11)–C(11)–C(12)	127·0 (14)	C(27)–C(28)–C(29)	119·6 (16)
C(11)–C(12)–C(13)	119·8 (11)	C(25)–C(30)–C(31)	110·5 (12)
C(11)–C(12)–C(17)	119·1 (16)	C(25)–C(30)–C(32)	109·9 (11)
C(13)–C(12)–C(17)	120·9 (14)	C(31)–C(30)–C(32)	110·6 (11)
O(2)–C(13)–C(12)	120·4 (11)	O(3)–C(33)–O(33)	124·2 (13)
O(2)–C(13)–C(14)	118·6 (13)	O(3)–C(33)–C(1)	112·4 (9)
C(12)–C(13)–C(14)	120·9 (11)	O(33)–C(33)–C(1)	123·3 (12)
C(13)–C(14)–C(15)	116·6 (14)	C(34)–S–C(35)	97·03*
C(13)–C(14)–C(19)	120·5 (10)	C(34)–S–O(37)	106·75*
C(15)–C(14)–C(19)	122·9 (12)	C(35)–S–O(37)	106·14*
C(14)–C(15)–C(16)	121·5 (12)	S–C(35)–C(36)	109·40*
C(15)–C(16)–C(17)	122·7 (11)		

* Rigid model for (*R*)-ethyl methyl sulfoxide.

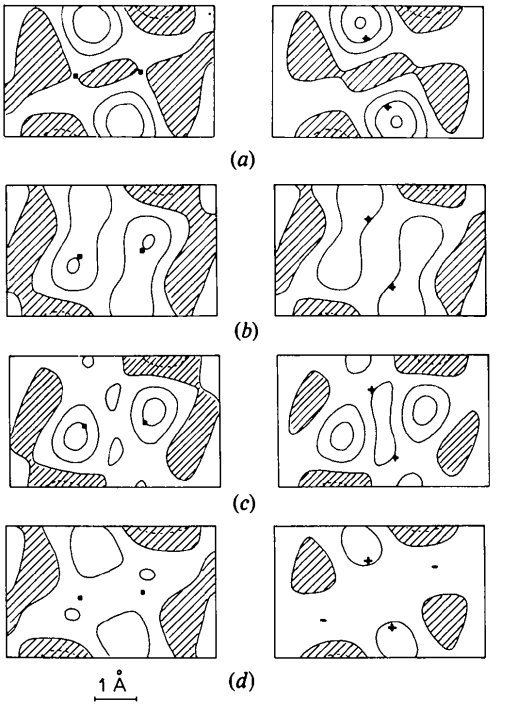

Fig. 3. Residual electron density within the cage. The sections are perpendicular to the crystallographic twofold axis and calculated from the F_c model (*M*)-TOT–(*R*)-EMSO/(*S*)-EMSO ($2:x_R:x_S$). Contour interval 1 e Å^{-3}, starting at zero contour. Shaded areas: negative density. The equation of the planes passing through the axially disordered S atoms can be expressed as $13{\cdot}538x - 6{\cdot}769y = D$ in direct space. The D value is 4·061 Å for the (*R*) enantiomer (S atoms at ■; left column) and 4·197 Å for the (*S*) enantiometer (S atoms at +; right column). The guest occupancy factor is $x_R + x_S = 0{\cdot}96$. The enantiomeric excess (%) of the (*R*) configuration is calculated as $(x_R - x_S)$. $100/(x_R + x_S)$: (*a*) 100%; (*b*) 83%; (*c*) 72%; (*d*) final residual density after refinement of the F_c model with e.e. = 83%. The S-atom positions labelled with + are those originally calculated with the *PCK*-6 program (Williams, 1972). The final refinement shifts these positions by 0·25 Å away from the twofold axis towards the region of the highest electron density shown in Fig. 3(*a*).

R to 0·049.* The positional and thermal parameters are reported in Tables 1 and 2. Bond distances and angles are in Table 3. A ΔF synthesis computed at this final stage of the analysis displayed a levelling of the electron density within the cage: the peak heights decreasing to 1·0 and 1·5 e $Å^{-3}$ at the non-equivalent positions of the S atoms (Fig. 3*d*). These values compare well with the maximum residual value of about 1 e $Å^{-3}$ calculated outside the cavity. One might argue from the residual positive electron density in the cage that the overall occupancy factor is still underestimated. However, further empirical adjustments of the population parameters did not seem meaningful under conditions where the refinement is certainly already limited by the approximations involved in the guest model (especially the assignment of a common isotropic thermal parameter to both enantiomers).

Discussion. Two types of static disorder are superimposed on the dynamic disorder and affect the electron-density distribution of the cage contents: (i) a space-averaged electron density resulting from the weighted contribution of enantiomeric molecules, and (ii) an orientational disorder to conform with the imposed twofold symmetry of the cage (see Fig. 4). Despite these severe disturbances the 'disordered' heavy atoms are fairly well resolved owing to their particular position in the guest skeleton. This favorable situation is unfortunately unique among the TOT clathrates that have been investigated so far.

It is possible to establish a host–guest configurational correlation on the basis of the known absolute configuration of TOT (Gerdil & Allemand, 1979). The sign of the optical rotation is noted upon dissolution of a single crystal of TOT and after complete racemization of the host the residual optical activity of the excess guest enantiomer can be measured. In the present case the (*R*) configuration could be correlated with the (−) isomer of ethyl methyl sulfoxide, in agreement with previous configuration assignments accomplished by other methods (Axelrod, Bickart, Goldstein, Green, Kjaer & Mislow, 1968; Pirkle & Beare, 1968).

The overall molecular packing is very similar to those of the 2-butanol (Allemand & Gerdil, 1981) and 2-bromobutane clathrates (Allemand & Gerdil, 1982). There are no significant host···guest contacts shorter than the sum of the respective van der Waals atomic radii. Moreover the contacts are so evenly distributed, in particular around the guest methyl groups, that only little motional freedom seems to be allowed to the caged molecule.

Financial support of this work by the Swiss National Science Foundation is gratefully acknowledged.

* Lists of structure factors, anisotropic thermal parameters and positions of H atoms have been deposited with the British Library Lending Division as Supplementary Publication No. SUP 36782 (11 pp.). Copies may be obtained through The Executive Secretary, International Union of Crystallography, 5 Abbey Square, Chester CH1 2HU, England.

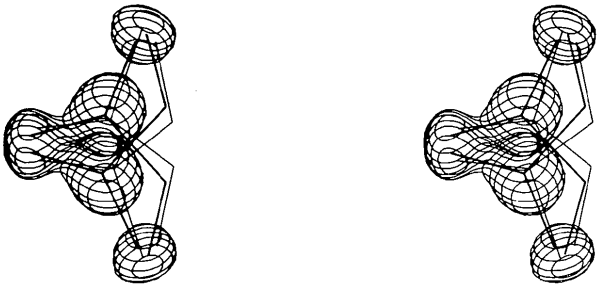

Fig. 4. Stereoview of the electron-density distribution of ethyl methyl sulfoxide in its average position of twofold disorder (calculated from a ΔF synthesis). The contours include about 90% of the total electron population. The composite density results from the space-averaged contribution of (*S*) and (*R*) enantiomers (thin and heavy lines, respectively) in the approximate ratio 1:11.

References

ALLEMAND, J. & GERDIL, R. (1981). *Cryst. Struct. Commun.* **10**, 33–40.

ALLEMAND, J. & GERDIL, R. (1982). *Acta Cryst.* B**38**, 1473–1476.

AXELROD, M., BICKART, P., GOLDSTEIN, M. L., GREEN, M. M., KJAER, A. & MISLOW, K. (1968). *Tetrahedron Lett.* pp. 3249–3252.

GERDIL, R. & ALLEMAND, J. (1979). *Tetrahedron Lett.* pp. 3499–3502.

GERDIL, R. & ALLEMAND, J. (1980). *Helv. Chim. Acta*, **63**, 1750–1753.

GERDIL, R., ALLEMAND, J. & BERNARDINELLI, G. (1981). *Acta Cryst.* A**37**, C92.

PIRKLE, W. H. & BEARE, S. D. (1968). *J. Am. Chem. Soc.* **90**, 6250–6251.

POWELL, H. M. (1964). *Non-Stoichiometric Compounds*, edited by L. MANDELCORN, pp. 469–480. New York: Academic Press.

SVINNING, T., MO, F. & BRUUN, T. (1976). *Acta Cryst.* B**32**, 759–764.

WILLIAMS, D. E. (1972). *Acta Cryst.* A**28**, 629–635.